Chapter

Use of Discrete-Time Forecast Modeling to Enhance Feedback Control and Physically Unrealizable Feedforward Control with Applications

Derrick K. Rollins

Abstract

When the manipulated variable (MV) has significantly large time delay in changing the control variable (CV), use of the currently measured CV in the feedback error can result in very deficient feedback control (FBC). However, control strategies that use forecast modeling to estimate future CV values and use them in the feedback error have the potential to control as well as a feedback controller with no MV deadtime using the measured value of CV. This work evaluates and compares FBC algorithms using discrete-time forecast modeling when MV has a large deadtime. When a feedforward control (FFC) law results in a physically unrealizable (PU) controller, the common approach is to use approximations to obtain a physically realizable feedforward controller. Using a discrete-time forecast modeling method, this work demonstrates an effective approach for PU FFC. The Smith Predictor is a popular control strategy when CV has measurement deadtime but not MV deadtime. The work demonstrates equivalency of this discrete-time forecast modeling approach to the Smith Predictor FBC approach. Thus, this work demonstrates effectiveness of the discrete-time forecast modeling approach for FBC with MV or DV deadtime and PU FFC.

Keywords: Model Predictive Control, Nonlinear Dynamic Modeling, Artificial Pancreas

1. Introduction

Modeling data is critical to the advancement of information and data science on many levels and in many areas. Accurately modeling data is often important to system monitoring, understanding, and control; and thus, ultimately to the advancement of technology.

A characteristic of data that that is not well understood, even by those in the physical sciences, is dynamic behavior. However, the behavior of Covid-19, which is inherently dynamic, has forced wide-spread conversations from even the non-science community about such terms as lag and deadtime. Just as understanding the attributes of Covid-19 dynamically can lead to intelligent and thus, safe behavior,

good decision making and preparation, and even save lives, the lack of understanding can do the opposite. Thus, the better our understanding of dynamic behavior is, physically and biologically, the better our understanding of data will be, leading only to better solutions to many problems facing society.

Forecast modeling is a type of predictive modeling that uses current and anticipated future input values to predict values for outputs in the future. For example, forecast modeling is used to predict the wind velocity in a certain region five days into the future. Another example is forecast modeling to predict the number of deaths caused by a virus a week into the future. This chapter focuses on the application of forecast modeling to enhance feedback control (FBC) and feedforward control (FFC) when the problem is physically unrealizable (PU).

A PU system is a mathematical phenomenon of a dynamic system. It occurs in two ways. The first one is when the order of the differential equation for the output is less than the order of the differential equation for the input. An example is the development of a FFC law determined from a load transfer function divided by the process transfer of a lower order. The second one is when an output depends on deadtime that has a negative value, in effect causing a dependence on future values of a time dependent variable(s). This also occurs in FFC when the load transfer function has a smaller deadtime than the process transfer function. The most common approach for addressing a PU system is to use approximation(s) to make it physically realizable. However, such approximations can lead to large modeling errors, thus leading to unacceptable control.

The dynamic modeling literature [1, 2] defines ***causality*** somewhat differently than the statistics literature. More specifically, "if a system['s] output depends on the future input values ... the system is noncausal [2]." **This definition is synonymous with PU**, it seems. In forecast modeling, all values of inputs are before the forecast distance in the future. They can be in the future, but not a distance beyond the forecast time. Another description for PU in the dynamic modeling literature is *improper transfer function*.

In FFC, MV is the output and depends on input changes. When MV has a deadtime of θ_{MV}, for example, it takes this time before a change in MV affects CV. Within this period, other inputs may change that impact CV before the change in MV does. An example is the control of blood glucose concentration (BGC) in type 1 diabetes. The deadtime for insulin infusion is much larger than the deadtime for carbohydrate consumption. The best approach for control of BGC is to consider the timing and the amount of carbohydrates consumed and to bolus this with a determined amount of insulin, a calculated amount of the time before the meal. This procedure is just a manual type of PU FFC practiced by people with type 1 diabetes.

The use of causality in the statistics literature seeks to distinguish it from correlation. Thus, in the statistics literature, causality is not focused exclusively on dynamic systems (e.g., only those with lag or deadtime) but a ***cause-and-effect*** relationship between input and output, that can be nondynamic [3]. For forecast modeling, ***cause-and-effect*** is not essential if the model is accurate. However, in control, ***cause-and-effect*** modeling is essential. A PU system does not have an exact solution which would be a continuous-time solution. However, a discrete-time solution can be determined directly from the PU continuous-time structure. Hence, this work uses highly structured discrete-time forecasting and FFC models.

1.1 Objective and contribution of the work

Moreover, the primary objective of this chapter is to apply a novel discrete-time forecasting modeling methodology to systems with large MV deadtime in FBC and PU FFC without physical realizable approximations. For this scope, FBC is

examined and evaluated under three prediction horizons: 1. None – Classical FBC that uses the currently measured value of CV [4, 5]; 2. θ_{MV} – Feedback Predictive Control (FBC) [6] and; greater than θ_{MV} – Model Predictive Control (MPC) [7, 8]. The Smith Predictor (SP) [9] is a novel FBC approach when $\theta_{MV} = 0$ and there is deadtime in the measurement of CV. This work shows that FBPC gives equivalent control of the SP, but also has the advantage that it is applicable when $\theta_{MV} > 0$, which the SP is not. In addition, this work reveals the detrimental use of the bias correction as given in the block diagram of the SP and used widely in process control [4]. Thus, this work proposes a better bias correction method. Finally, this works presents a novel discrete-time PU FFC algorithm that is multiple-input and single-output and hence, is able to treat complex multiple-input feedforward model structures. Although MPC is a FBC approach, comparison is made to illustrate the potential improvement of FFPC over model-based predictive FBC.

2. Physically unrealizable

Physical unrealizability (PU) is an anomaly that is strictly an artifact of a dynamic system. A dynamic system has at least one process state (i.e., output or response) that does not change to its new value immediately when input changes occur that cause its value (i.e., level) to change. This behavior contrasts with a nondynamic system that changes to its new state immediately when inputs change (also, called "disturbances").

There are two basic dynamic phenomena – time lag and time delay (also called "dead time") which are shown in **Figure 1**. This figure illustrates nondynamic and dynamic relationships for the response, y, to a step change in the input, x, occurring

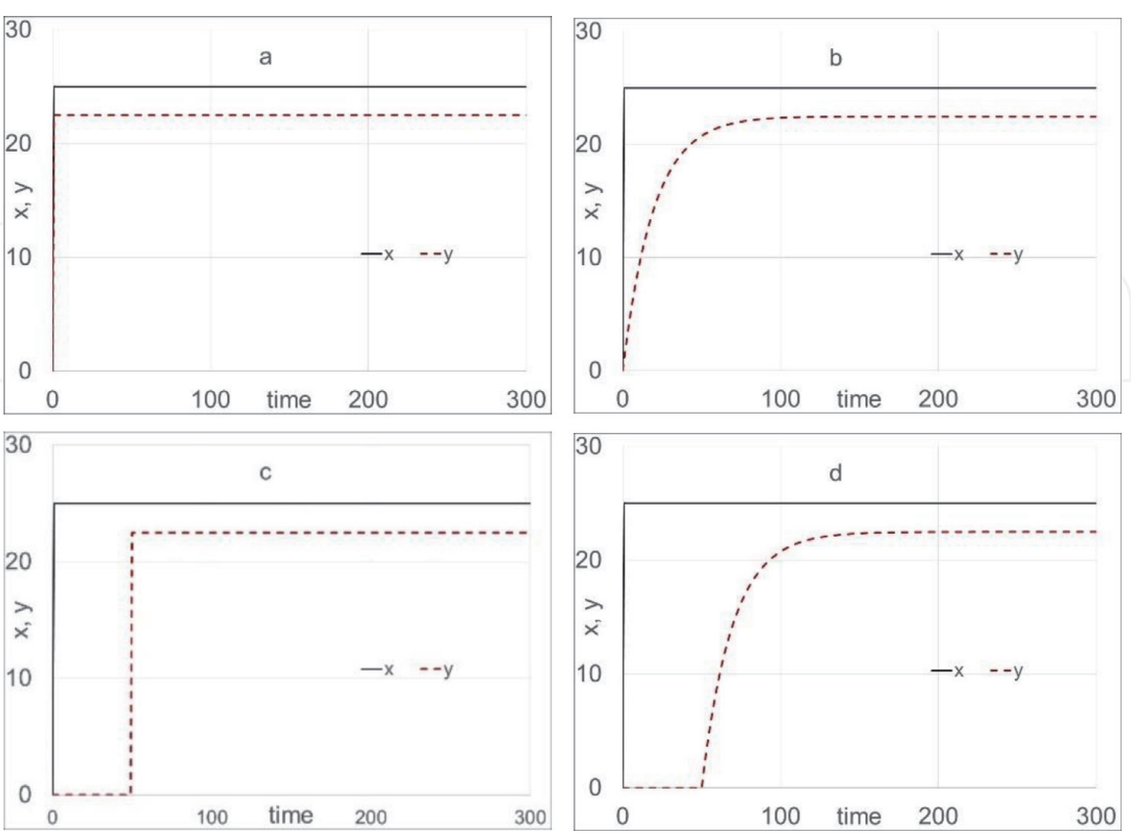

Figure 1.
Response y *to a step change in* x*: a. nondynamic; b. lag; c. time delay and; d. lag and time delay.*

at time (t) = 0. As shown, for the nondynamic response (a), y changes immediately to its new steady state value. Lag (b) is shown by the change in y starting to occur at t = 0, but monotonically increasing over time to its new steady state value. Time delay (c) is shown by the change in y to its new value occurring θ time later. Lag and time delay (d) are shown by y starting to change θ time later and then monotonically increasing over time to its new steady state value. "Everyday" examples of nondynamic changes are eyes opening (x) and immediate sight (y) and turning on the radio in a car (x) and hearing it (y) immediately. A dynamic time delay example is lightening occurring very far away. It occurs when one sees the lightening, but the thunder is delayed and occurs at a significant time after seeing the lightening. It does not build up to its final value, there is just a big boom that occurs, essentially, at once. A dynamic change with lag occurs when a person has been out in the cold for a while and their skin temperature is quite cold and when they move to a warmer environment, their temperature starts to rise but it takes time for the temperature to reach its new level in this warmer environment.

When a system is dynamic, its mass and/or internal energy changes over time, being driven to a new state due to input changes, arriving there at a time different than when the input was changed. Mathematically (and theoretically) this is seen as a time-order differential equation. Such an equation is given in terms of input x and output y in Eq. (1).

$$\begin{aligned} &a_n \frac{d^n y(t)}{dt^n} + a_{n-1} \frac{d^{n-1} y(t)}{dt^{n-1}} + \cdots + a_1 \frac{dy(t)}{dt} + a_0 y(t) = \\ &b_m \frac{d^m x(t-\theta)}{dt^m} + b_{m-1} \frac{d^{m-1} x(t-\theta)}{dt^{m-1}} + \cdots + b_1 \frac{dx(t-\theta)}{dt} + b_0 x(t-\theta) \end{aligned} \tag{1}$$

The dynamic form represented by Eq. (1) is PU if $n < m$, if θ is negative, or if both are true. More specifically, the output, y, which depends on the input, x, cannot have a time dependent derivative structure that is of lower order than the variable that causes it to change. The response of a system to a disturbance also cannot have negative time delay. A system cannot respond to a disturbance before it occurs. There is no true solution for these conditions.

However, there are ways to address these PU cases in practice. For the first case, $n < m$, discrete-time backwards different derivatives can be used to approximate the continuous-time derivatives. This approach should provide adequate accuracy when the sampling time is constant and sufficiently small, and sensor noise is not too great. Eq. (2) illustrates this approximation when m = 2, n = 1, a constant sampling time, Δt, and with θ = 0 (for simplicity). Note, since $y(t)$ cannot be immediately affected by $x(t)$, $x_{t\text{-}\Delta t}$ is used to approximate $x(t)$.

$$\begin{aligned} &a_1 \frac{dy(t)}{dt^n} + a_0 y(t) = b_2 \frac{d^2 x(t)}{dt^2} + b_1 \frac{dx(t)}{dt} + b_0 x(t) \\ &\Rightarrow y_t \approx \frac{y_{t-\Delta t} + \left(\frac{b_2}{\Delta t} + b_1 + b_0 \Delta t\right) x_{t-\Delta t} - \left(\frac{2b_2}{\Delta t} + b_1\right) x_{t-2\Delta t} + \frac{b_2}{\Delta t} x_{t-3\Delta t}}{1 + a_0 \Delta t} \end{aligned} \tag{2}$$

Thus, digital and sensor technologies, among other advancements, have significantly contributed to an ability to approximate Eq. (1) when $n < m$.

For the other case, i.e., when the time delay is a negative value such as a -5Δt (e.g., in FFC when deadtime for the disturbance variable (θ_{DV}) is smaller than the deadtime for the manipulated variable (θ_{MV})), Eq. (2) becomes

$$a_1\frac{dy(t)}{dt^n}+a_0y(t)=b_2\frac{d^2x(t+5\Delta t)}{dt^2}+b_1\frac{dx(t+5\Delta t)}{dt}+b_0x(t+5\Delta t)$$

$$\Rightarrow y_t\approx\frac{y_{t-\Delta t}+\left(\frac{b_2}{\Delta t}+b_1+b_0\Delta t\right)x_{t+5\Delta t-\Delta t}-\left(\frac{2b_2}{\Delta t}+b_1\right)x_{t+5\Delta t-2\Delta t}+\frac{b_2}{\Delta t}x_{t+5\Delta t-3\Delta t}}{1+a_0\Delta t}$$

$$=\frac{y_{t-\Delta t}+\left(\frac{b_2}{\Delta t}+b_1+b_0\Delta t\right)x_{t+4\Delta t}-\left(\frac{2b_2}{\Delta t}+b_1\right)x_{t+3\Delta t}+\frac{b_2}{\Delta t}x_{t+2\Delta t}}{1+a_0\Delta t} \tag{3}$$

Thus, as shown by Eq. (3), the output depends on future values of the input. However, discrete-time modeling provides a means to express an approximate solution in a PU form where knowledge of future changes allows approximation of the output. An example where this type of approximation is applied, is the control of blood glucose concentration (BGC) for people with type 1 diabetes [10]. The manipulated variable (MV) for the automatic regulation of the exogenous insulin infusion from a servo-mechanical pump can have a deadtime of 60 minutes and carbohydrates from meals can have a deadtime of 30 minutes [11], resulting in $x(t)$ becoming $x(t + 30)$ in the numerator of the FFC law, with *MV* as the output variable. Moreover, for these values, a change in insulin flow rate will take one hour to begin to lower BGC. During this period, eating can increase BGC. People with type 1 diabetes understand this phenomenon and will bolus their insulin infusion, based on when they will eat and how many carbohydrates they will eat. This is called "a meal announcement" [12, 13]. But just as this idea is applied to carbohydrates, it can be applied to other variables with dead times less than *MV* such as stress, exercise, etc. As one can imagine, the relationships of such a set of variables on BGC is quite complex and accurately modeling their relationships and automatic feedback/feedforward control (FBFFC), with accurate announcements, appears to be the most viable one for success. In the content to follow, we focus on dynamic modeling with application to feedback control (FBC) and FFC when time delay in MV is significantly larger than time delay in disturbances. For this situation, when CV is the output, forecast modeling is necessary and when MV is the output, future announcement (i.e., knowledge) is needed for any variable with a dead time less than that of MV.

3. Discrete-time forecast dynamic modeling

Accurate forecast dynamic modeling in the context of process control has two critical applications. One is accurately *forecasting* CV at least θ_{MV} distance into the future, depending on the type of model-based control algorithm being used in FBC. The other one is an accurate *cause-and-effect* model for CV that is inverted for determining MV as a function of disturbances in FFC. Empirical modeling methods (EMM) (i.e., the so-called "data-driven" methods such as linear regression and artificial neural networks) are fit to a correlation structure and should not be used for *cause-and-effect* modeling unless the modeling data are generated from a statistical experimental design covering the full range of the operating (i.e., input) space. This input space will be orthogonal and prevent extrapolation, which is risky for EM. For "freely existing data" or any data not generated from a statistical experimental design, accurate EM for CV forecasting is possible. However, when modeling data are not generated by a statistical experimental design, it would not be wise

to use EM when *cause-and-effect* modeling is needed since EMM are data driven and not knowledge driven, rely on high levels of parametrization, do not have structures or parameters that are physically interpretable based on first principles modeling, and are typically very risky for, even slight, extrapolation. In contrast, first principles model structures are: 1. nonlinear and thus, naturally break down correlation structures in the input data; 2. have physically interpretable parameters; and 3. often physical constraints with a theoretical basis. Nonetheless, theoretically based modeling of real data outside a controlled environment such as a lab, is often some combination of empiricism and first principles knowledge, which is essentially a "hybrid model" that is often called "gray box" or "semi-empirical" models. Models that are fully theoretical in derivation and structure but use data to obtain unknown physically interpretable model parameters, are classified in this document as semi-theoretical models.

Theoretically structured dynamic systems can be linearized (i.e., approximated) in time dependent variables (i.e., $x = x(t)$) while maintaining their time derivative structures (i.e., the order of derivatives will remain intact) and physical parametrization. For example, Eq. (4) represents the result of a dynamic overall mass balance on a process tank with one inlet stream with flow rate, $q_1(t)$, and one outlet stream though a hand valve with flow rate, $q(t) = h^2(t)/\mathrm{R_v}$, where h is the tank level, R_v is the resistance to flow through the valve, and A is the cross-sectional area of the tank. The density and temperature of the fluid in the tank is constant in this example. Using a 1st order Taylor Series approximation to linearize all time dependent variables in Eq. (4), gives the solution in Eq. (5), where the "′" represents a variable as a deviation from its initial steady state at $t = 0$.

$$A\frac{dh(t)}{dt} = q_1(t) - R_V^{-1}h^2(t) \tag{4}$$

$$A\frac{dh'(t)}{dt} = q_1'(t) - 2R_V^{-1}h(0)h'(t) \tag{5}$$

Rearranging Eq. (5) into the form of Eq. (1) gives:

$$\begin{aligned} a_1\frac{dh'(t)}{dt} + a_0h'(t) &= b_0q_1'(t) \\ \tau\frac{dh'(t)}{dt} + h'(t) &= Kq_1'(t) \end{aligned} \tag{6}$$

where $a_1 = A\left[2R_V^{-1}h(0)\right]^{-1} = \tau,\ a_0 = 1\ and\ b_0 = K = \left[2R_V^{-1}h(0)\right]^{-1}$. Eq. (6) is a first-order dynamic relationship with time constant, τ, and steady-state gain, K, and is represented in "standard form [4, 5]." Many dynamic processes can be approximated accurately by either a first-order-plus-deadtime (FOPDT) or second-order-plus-deadtime (SOPDT) structure [4, 5].

Eq. (7) gives a second-order version of Eq. (1) for inputs x_i', $i = 1, \ldots, p$, and unity gain, with y replaced by v_i'. Thus, Eq. (7) represents the dynamic response due to x_i', in the units of x_i'. Eq. (8) represent the dynamic response of y as a function of $v_i's$ where $f(\boldsymbol{V})$ is an unrestricted mathematical function that maps each v_i' to the units of the output variable in standard form. Thus, it is $f(\boldsymbol{V})$ that transforms the linear dynamic inputs into the nonlinear dynamic and static response for the output y.

$$\tau_i^2\frac{d^2v_i(t)}{dt^2} + 2\tau_i\zeta_i\frac{dv_i(t)}{dt} + v_i(t) = \tau_{ai}\frac{dx_i(t-\theta_i)}{dt} + x_i(t-\theta_i) \tag{7}$$

$$y(t) = f(\mathrm{V}(t)) + \varepsilon(t) = \eta(t) + \varepsilon(t) \tag{8}$$

where $\mathrm{V}(t)$ is a vector of the $v_i''s$ and the estimate of $y(t)$, denoted as $\hat{y}(t)$, is equal to the estimate of $\eta(t)$, $\hat{\eta}(t)$. This hybrid dynamic modeling structure is called a Wiener network [14] and is in a class of structures that are called "block-oriented models." The block diagram for this network is shown in **Figure 2**.

Rollins, et al. [15] developed a multiple-input, single-output, discrete-time, nonlinear Wiener dynamic approach using backwards difference derivatives based on Eqs. (7) and (8). Using a backward difference approximation applied to a sampling interval of Δt, an approximate discrete-time form of Eq. (7) is obtained (for p inputs):

$$v_{i,t} = \delta_{1,i} v_{i,t-\Delta t} + \delta_{2,i} v_{i,t-2\Delta t} + \omega_{1,i} x_{i,t-\theta_i-\Delta t} + \omega_{2,i} x_{i,t-\theta_i-2\Delta t} \tag{9}$$

where $\omega_{2,i} = 1 - \delta_{1,i} - \delta_{2,i} - \omega_{1,i}$ to satisfy the unity gain constraint with

$$\delta_{1,i} = \frac{2\tau_i^2 + 2\tau_i\zeta_i\Delta t}{\tau_i^2 + 2\tau_i\zeta_i\Delta t + \Delta t^2} \tag{10}$$

$$\delta_{2,i} = \frac{-\tau_i^2}{\tau_i^2 + 2\tau_i\zeta_i\Delta t + \Delta t^2} \tag{11}$$

$$\omega_{1,i} = \frac{(\tau_{ai} + \Delta t)\Delta t}{\tau_i^2 + 2\tau_i\zeta_i\Delta t + \Delta t^2} \tag{12}$$

After obtaining $v_{i,t}$ for each input i ($i = p$ is MV), the modeled output value is determined by substituting these results into $f(\boldsymbol{V})$, such as

$$\begin{aligned} \eta_t = f(\mathrm{V}) = a_0 + a_1 v_{1,t} + \cdots + a_p v_{p,t} + b_1 v_{1,t}^2 + \cdots + b_p v_{p,t}^2 \\ + c_{1,2} v_{1,t} v_{2,t} + \cdots + c_{p-1,p} v_{p-1,t} v_{p,t} \end{aligned} \tag{13}$$

Modification of Eq. (13) for forecasting $\eta(t)$ a distance θ_{MV} into the future with $p = 3$, for example, gives

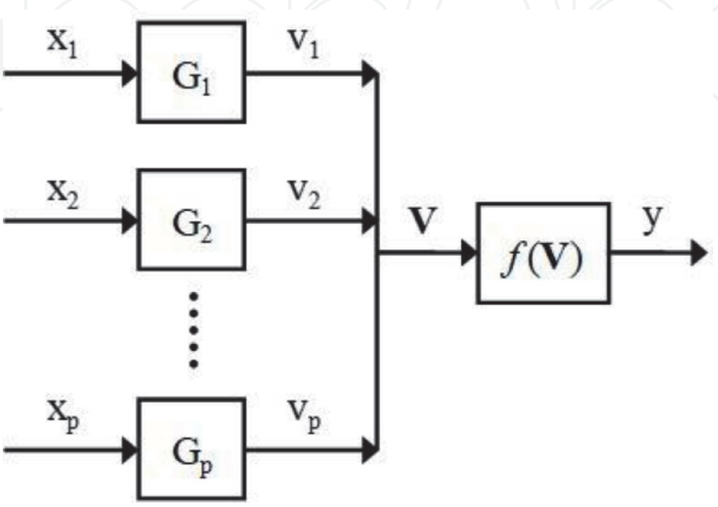

Figure 2.
Block diagram for the wiener network with p *inputs and one output. Each input,* x_i, *is passed through their own unity gain linear dynamic block,* G_i, *after which these unobservable intermediate outputs are collected and passed through a single unrestricted static gain function,* f(**V**), *to produce the output,* y.

$$\eta_{t+\theta_{MV}} = a_0 + a_1 v_{1,t+\theta_{MV}} + \cdots + a_3 v_{3,t+\theta_{MV}} + b_1 v_{1,t+\theta_{MV}}^2 + \cdots + b_3 v_{3,t+\theta_{MV}}^2 + c_{1,2} v_{1,t+\theta_{MV}} v_{2,t+\theta_{MV}} + \cdots + c_{2,3} v_{2,t+\theta_{MV}} v_{3,t+\theta_{MV}} \tag{14}$$

where a_i, b_i, and $c_{i,j}$, denote the linear, quadratic and interaction parameters for i = 1, 2, 3 and j = 2 and 3, and

$$v_{1,t+\theta_{MV}} = \delta_{1,1} v_{1,t+\theta_{MV}-\Delta t} + \delta_{2,1} v_{1,t+\theta_{MV}-2\Delta t} + \omega_{1,1} x_{1,t+\theta_{MV}-\theta_{DV_1}-\Delta t} + \omega_{2,1} x_{1,t+\theta_{MV}-\theta_{DV_1}-2\Delta t} \tag{15}$$

$$v_{2,t+\theta_{MV}} = \delta_{1,2} v_{2,\theta_{MV}-\Delta t} + \delta_{2,2} v_{2,t+\theta_{MV}-2\Delta t} + \omega_{1,2} x_{2,t+\theta_{MV}-\theta_{DV_2}-\Delta t} + \omega_{2,2} x_{2,t+\theta_{MV}-\theta_{DV2}-2\Delta t} \tag{16}$$

$$\begin{aligned} v_{3,t+\theta_{MV}} &= \delta_{1,3} v_{3,t+\theta_{MV}-\Delta t} + \delta_{2,3} v_{3,t+\theta_{MV}-2\Delta t} \\ &+ \omega_{1,3} x_{3,t+\theta_{MV}-\theta_{MV}-\Delta t} + \omega_{2,3} x_{3,t+\theta_{MV}-\theta_{MV}-2\Delta t} \\ &= \delta_{1,3} v_{3,t+\theta_{MV}-\Delta t} + \delta_{2,3} v_{3,t+\theta_{MV}-2\Delta t} + \omega_{1,3} x_{3,t-\Delta t} + \omega_{2,3} x_{3,t-2\Delta t} \end{aligned} \tag{17}$$

where the θ's are integer multiples of Δt. Depending on the rate of change of CV, forecast accuracy (and hence, control) can suffer significantly by setting θ_{MV} - θ_{DV} to zero. Developers of BGC devices that use current sensor glucose measurements in the feedback error restrict these devices for use only during long sleeping periods when BGC changes very slowly. For an application such as automatic BGC control, with a very large deadtime for MV and many disturbances with smaller deadtime than MV, that are nonlinear and interactive, the required accuracy for forecasting BGC is quite challenging. However, as health monitoring sensor technology continues to advance, forecast modeling accuracy continues to improve. The strengths of the method presented in this chapter are the use of dynamic structures that are embedded in first principles modeling; that is, they have physically interpretable parameters embedded in highly nonlinear structures (Eqs. (10)–(12)) with physical constraints such as $\omega_{2,i} = 1 - \delta_{1,i} - \delta_{2,i} - \omega_{1,i}$, $\tau_i > 0$ and $\zeta_i > 0$, for all i. While the method has these strengths for forecasting [16, 17], these strengths are quite critical in FFC applications where *cause-and-effect* modeling is essential. Next PU is examined from a control perspective – FBC first and then feedback feedforward (FBFFC).

4. FBC when θ_{MV} is large

As discussed above, a change in MV will not affect CV until θ_{MV} time into the future. When θ_{MV} is 0, the feedback error for FBC is, rightly, $e_t = Y^{set} - y_t$, where y_t is the measured value of CV at the current time, t. When θ_{MV} is not 0, the equivalent feedback error is $e_t = Y^{set} - y_{t+\boldsymbol{\theta MV}}$ which is unknown because $y_{t+\boldsymbol{\theta MV}}$ is not obtained until time t + θ_{MV}. This section describes and compares three FBC approaches when θ_{MV} is not 0. The first one is classical FBC [4, 5] which uses $e_t = Y^{set} - y_t$. The second one is feedback predictive control (FBPC) [6] which uses $e_t = Y^{set} - \hat{y}_{t+\theta_{MV}}$. The third one is model predictive control (MPC) [18–20]. The MPC control law is for CV to be equal to Y^{set}, J time steps after t + θ_{MV} while holding the current value of MV fixed [4]. Thus, J is the only controller tuning parameter for MPC. More specifically, its feedback error is: $e_t = Y^{set} - \hat{y}_{t+\theta_{MV}+J\Delta t}$.Hence, the MPC prediction horizon is longer than FBPC by the amount $J\Delta t$. For MPC, the optimal value of $J\Delta t$ will tend to increase as the time lag of y_t increases for changes in MV. Since forecasting accuracy

typically decreases as the distance into the future increases, MPC control can significantly deteriorate as $J\Delta t$ increases.

These three control algorithms were compared by [6] in their ability to automatically control CV for a true FOPDT process with K = 1, τ = 10 and 50 min, θ_{MV} = 3 min, and a sampling time, Δt, equal to 1 min. FBPC and FBC were PI-Controllers with tuning parameters to give the best response with little, to no, overshoot for a unit step change in the set point at time t = 0.

Figure 3 presents the results of this study found in [6]. As shown, CV (y) is on the left and MV (M) is on the right. The top row represents τ = 10 (J = 3, 8, and 20) and the bottom row represents τ = 50 (J = 8, 20, and 30). As shown, as J decreases, y reaches the set point faster and overshoots it for the lowest values of J. FBPC reaches the set point much faster than MPC, even when MPC overshoots the set point. As τ increases, MPC takes longer to reach the set point, but this is not the case for FBPC and FBC. FBC reaches the set point faster without overshooting than MPC for the case with the larger τ. Moreover, depending on J and τ, FBC and MPC can reach the set point about the same time without overshooting the set point. However, FBPC has a faster response and reaches the set point much earlier than FBC and MPC in all cases. MV for FBPC has an initial "kick" much greater than FBC or MPC. However, its MV quickly drops below that of FBC and MPC and has significantly less movement in both cases as shown in **Figure 3**. Thus, as expected, because of the longer control horizon, which increases as τ increases, MPC responded slower than FBPC in reaching and staying at the new set point. Similar conclusions were seen in a comparison of FBPC and MPC in this article [6] for a simulated CSTR. Nonetheless, the main conclusion is that there are model-based forecasting FBC algorithms that are viable alternative to classical FBC when θ_{MV} is appreciably large.

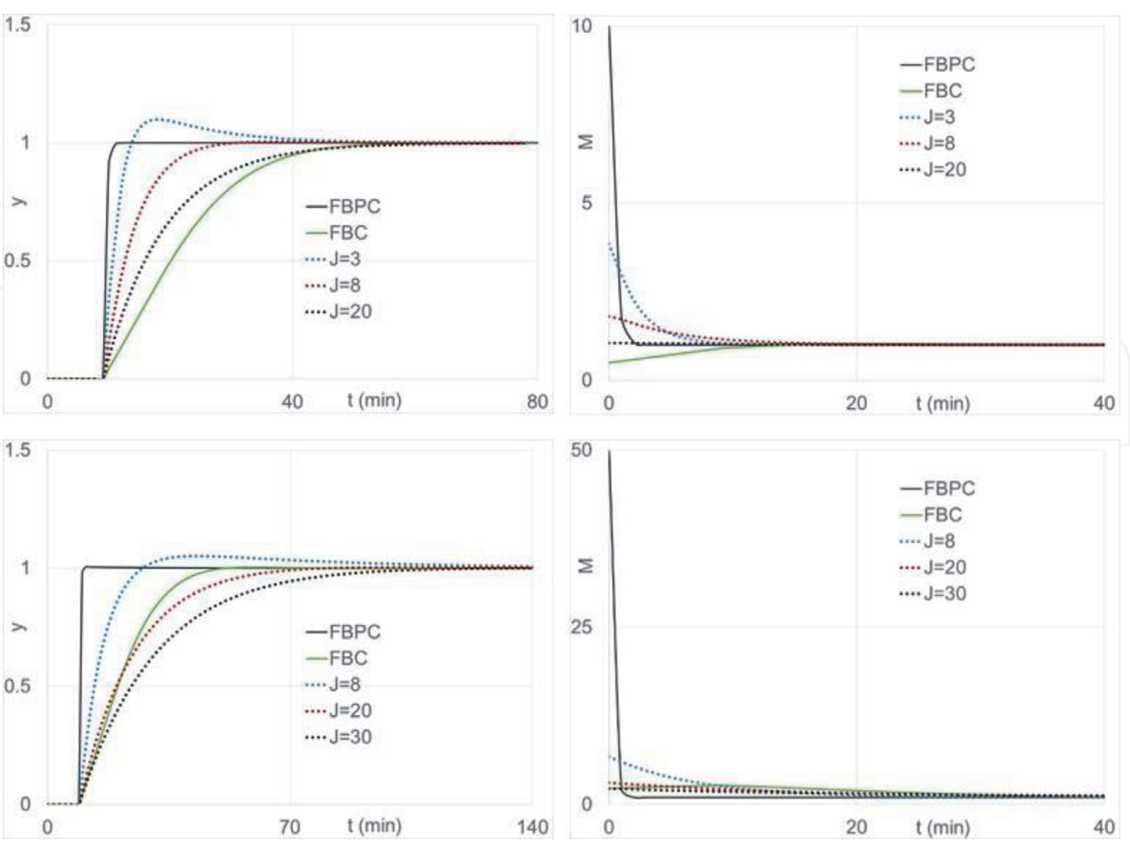

Figure 3.
CV (y) responses (left panels) and MV (M) changes (right panels) for FBPC, FBC and MPC for the FOPDT process. The top case is for τ = 10 (for MPC with J = 3, 8, and 20) and the bottom one is for τ = 50 (for MPC with J = 8, 20, and 30) [6].

5. FFC when θ_{MV} is large

All classical process control textbooks (e.g., [4, 5]) derive the FFC algorithm from a block diagram and give the FFC transfer function for each DV, G_f, as $-G_{DV}/G_{MV}$. The outputs from each G_f are added together to form the multiple-disturbance feedforward control law. An example when both G_{DV} and G_{MV} are FOPDT is:

$$G_f = -\frac{G_{DV}}{G_{MV}} = -\frac{\frac{K_{DV}e^{-\theta_{DV}S}}{\tau_{DV}s+1}}{\frac{K_{MV}e^{-\theta_{MV}S}}{\tau_{MV}s+1}} = -\frac{K_{DV}}{K_{MV}}\frac{\tau_{MV}s+1}{\tau_{DV}s+1}e^{(\theta_{MV}-\theta_{DV})S} = -\frac{K_{DV}}{K_{MV}}\frac{\tau_{MV}s+1}{\tau_{DV}s+1}e^{\Delta\theta S} \tag{18}$$

Thus, G_f will be PU when $\theta_{MV} > \theta_{DV}$, i.e., when $\Delta\theta > 0$. Typically, this limitation is addressed by just setting $\Delta\theta$ to 0 or increasing τ_{MV} to $\tau_{MV} + \Delta\theta$ and setting $e^{\Delta\theta S}$ to 1 [4]. This approximation is usually acceptable when $\Delta\theta$ is small, as commonly found in chemical processes. However, modern applications of process control have gone beyond chemical processes to biological processes where transport is cellular, slow, and complex (i.e., not well understood). A common example is exogenous insulin taken by people with diabetes as mentioned above [21]. Insulin deadtime is significantly greater than the deadtime for carbohydrate intake and other disturbances. Recent advancements in activity trackers measure multiple variables that likely affect BGC, and most, if not, all have a smaller deadtime than insulin [15–17].

Process Control textbooks commonly describe additive and linear dynamic FFC and present the algorithms in the continuous-time Laplace (s-) domain. This section presents a FFC approach that is: 1. given in the time domain; 2. discrete-time; 3. able to treat all types of non-additive behavior as well as nonlinear dynamic and static behavior and; 4. combines all disturbances functionally into one FFC law (i.e., all the DV's enter one FFC equation). A block diagram of this FFC approach based on the Wiener network is given in **Figure 4**. As shown, the modeled disturbances are

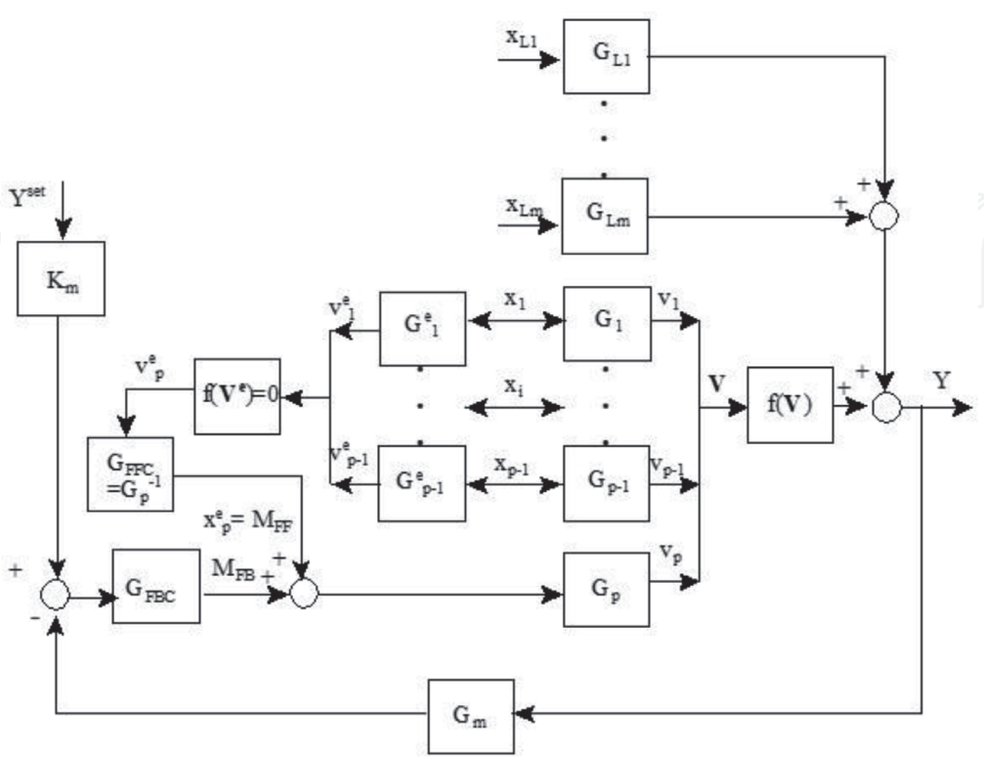

Figure 4.
Multiple-input FBC/FFC block diagram for a p*-input wiener network FFC model [22].*

x_1 to x_{p-1} and x_p is MV. Inputs x_1 to x_{p-1} pass through their dynamic blocks to produce v_1 to v_{p-1}. The FFC law associated with **Figure 4** is:

$$e_{ffc} = (Y^{set} - f(V^e))|_{x_p^e} = 0 \tag{19}$$

where $f(V^e)$ is defined in Eq, (8) with the superscript e associating it with the FFC law, i.e., $x_p^e = x_{MV}^e =$ value of MV that makes $e_{ffc} = 0$, and thus, satisfying Eq. (19).

For $p = 2$, i.e., one disturbance and MV, and FOPDT structures for both inputs, and application of linear forms for Eq. (13) (for simplicity) into Eq. (19) gives:

$$\begin{aligned} e_{ffc} &= (Y^{set} - a_0 - a_1 v_{1,t} - a_2 v_{2,t})|_{x_2} = Y^{set} - a_0 \\ &\quad - a_1[\delta_{1,1} v_{1,t+\theta_{MV}-\Delta t} + \delta_{2,1} v_{1,t+\theta_{MV}-2\Delta t} + \omega_{1,1} x_{1,t+\Delta\theta-\Delta t} + \omega_{2,1} x_{1,t+\Delta\theta-2\Delta t}] \\ &\quad - a_2[\delta_{1,2} v_{2,t+\theta_{MV}-\Delta t} + \delta_{2,2} v_{2,t+\theta_{MV}-2\Delta t} + \omega_{1,2} x_{2,t-\Delta t} + \omega_{2,2} x_{2,t-2\Delta t}] = 0 \\ \Rightarrow x_{2,t-\Delta t} &= x_{MV,t-\Delta t} = \frac{1}{\omega_{1,2}}(a_0 - Y^{set} \\ &\quad + a_1[\delta_{1,1} v_{1,t+\theta_{MV}-\Delta t} + \delta_{2,1} v_{1,t+\theta_{MV}-2\Delta t} + \omega_{1,1} x_{1,t+\Delta\theta-\Delta t} + \omega_{2,1} x_{1,t+\Delta\theta-2\Delta t}] \\ &\quad + a_2[\delta_{1,2} v_{2,t+\theta_{MV}-\Delta t} + \delta_{2,2} v_{2,t+\theta_{MV}-2\Delta t} + \omega_{2,2} x_{2,t-2\Delta t}]) \end{aligned} \tag{20}$$

Eq. (20) gives an explicit solution for the FFC signal, x_{MV}, in this example. When $f(\boldsymbol{V})$ has terms higher than first order, numerical root solving methods may be required to find x_{MV}, as illustrated in [22].

Eq. (20) is evaluated now to determine if it can meet the standard of perfect control for x_1 load changes. For a frame of reference, MPC is also included in this study although it is a FBC method. For this example, $Y^{set} = 100$ and remains constant. Input changes are made in $x_1(t)$ and its dynamic response to these input changes, $v_1(t)$, are given in **Figure 5**. The tuning parameter for MPC, J, has values of 1, 2 and 10. The model parameters are: $a_1 = 1$, $\tau_1 = 5$ min, $\theta_1 = 5$ min; $a_2 = -1$, $\tau_2 = 10$ min, $\theta_2 = 10$ min; and the sampling time, $\Delta t = 1$ min. The results for CV and MV for both FFPC and MPC are given in **Figure 5**. FFPC gives perfect control, as anticipated, and MPC does not, as anticipated. The response of MV that gives perfect control is the heavy black line in **Figure 5**. MPC with $J = 1$ appears to match the FFPC MV profile the best in terms of shape and time of changes, but it is also the most extreme. Thus, this example illustrates the ability of FFPC to meet the requirement of theoretically perfect control. **Figure 6** gives a general multiple-input, block-oriented model FBFF block diagram similar to the one in **Figure 4**. For more information see [13].

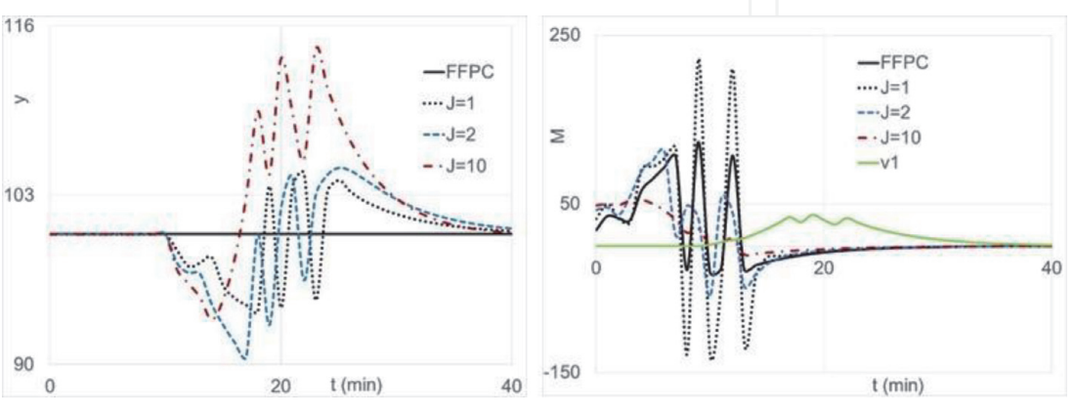

Figure 5.
CV (y) responses (left plot) and MV (M) *changes (right plot) for FFPC and MPC (J = 1, 2, and 10).* M = x_2 *for FFPC and MPC, and* M = v_1 *for the DV (i.e.,* x_1*) [13].*

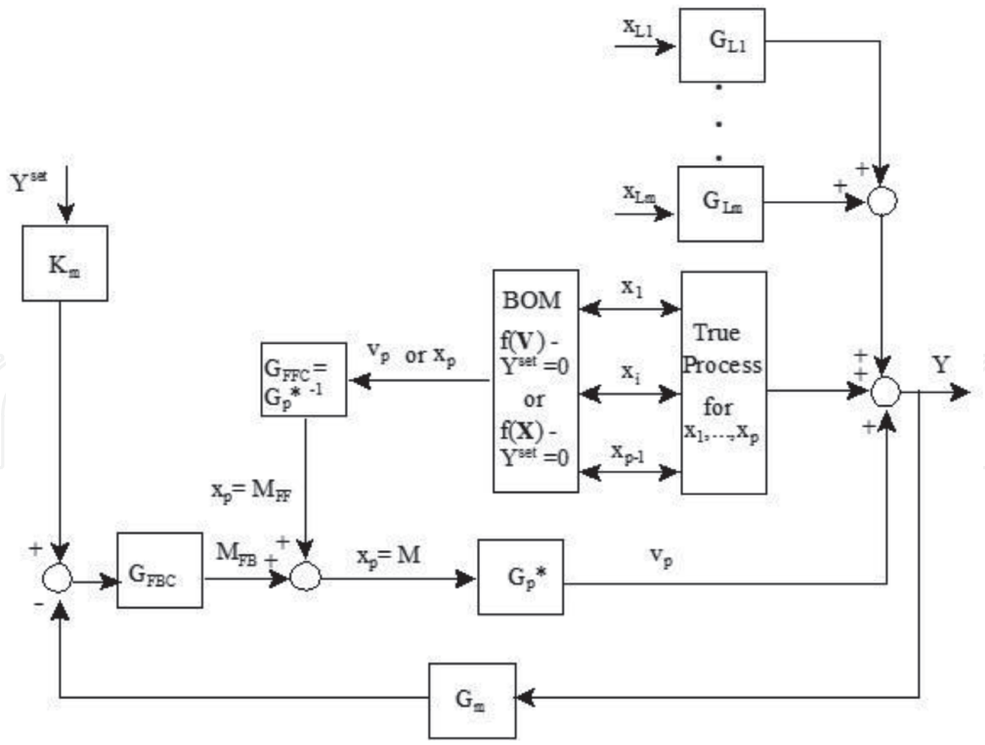

Figure 6.
A general BOM FBFF block diagram shown with m *loads and* p *FFC variables [8].*

FFPC is now evaluated on the *in silico* continuous stirred tank reactor (CSTR) in **Figure** 7 and described in [13] and taken from [5] with some minor modifications. This study has two DVs – feed composition, C_{Ai} (x_1), and temperature of the coolant entering the jacket, T_{Ci} (x_2)). MV is the flowrate of the coolant entering the jacket, F_C (x_3). The output (CV) is the measured tank temperature, T_m (y). The model for each input is SOPDT, as shown in Eq. (7). The output, y, follows Eq. (8) and measurement noise was added to the true tank temperature (T) to produce T_m. Modeling this process was an application of Eqs. (9)–(17) with $\theta_1 = \theta_2 = 5$ seconds (s) and $\theta_3 = \theta_{MV} = 10\ s$. Thus, $\Delta\theta = 5\ s$ for each input and both are PU in the FFC law. Therefore, the objective of this study is to compare announcement of input changes 5 s ahead versus no announcement.

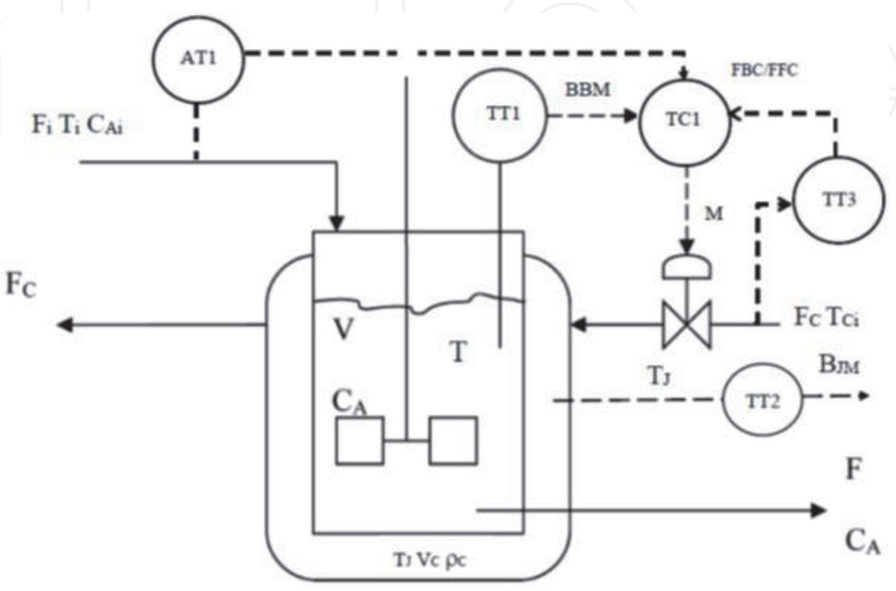

Figure 7.
Flow diagram of the CSTR in the in silico *study.*

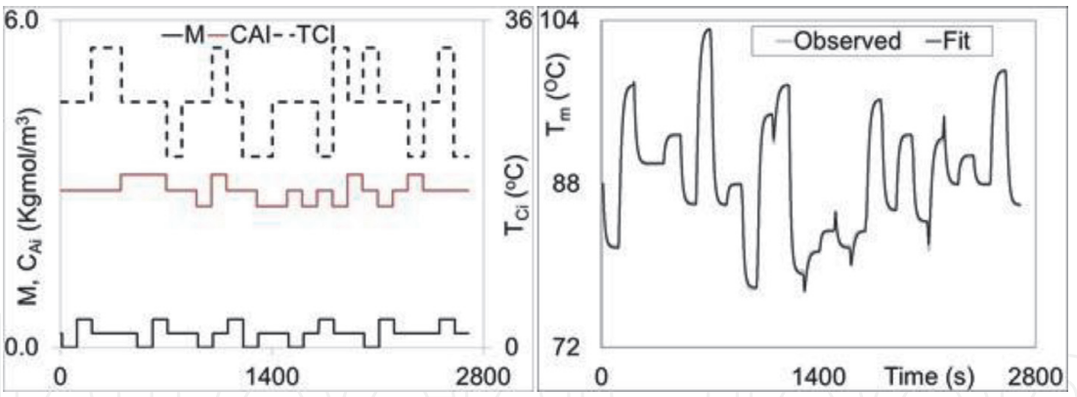

Figure 8.
Input sequences (left plot) C_{Ai} (x_1), T_{Ci} (x_2) *and M* (x_3) *and its wiener model fit (right plot).*

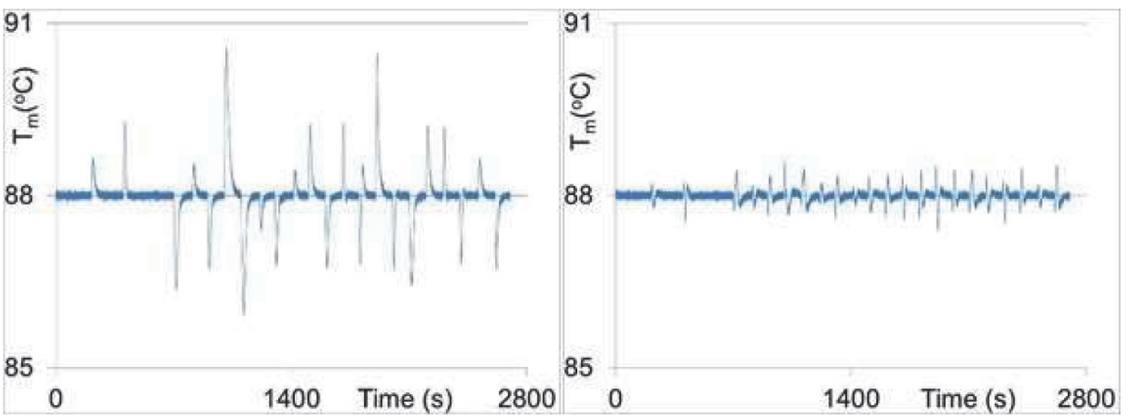

Figure 9.
The effect of T_{ci} *and* C_{Ai} *announcement on tank temperature* T_m *for FFPC (left plot is without announcement for both and right plot with announcements for both).*

A proportional-integral (PI) feedback controller was implemented in this study. Thus, FBPC was not used for FBC in any case to evaluate FFPC exclusive of FBPC. For this controller K_C = 1.40, τ_I = 11.0 and M_{FB} is the FBC signal to the control valve. $M_{FF} = x_3^e = x_{MV}^e$, is the FFPC signal. Thus, the signal to the valve, M, in **Figure 7** is $M = M_{FB} + M_{FF}$. The input sequence used for training the model is given in **Figure 8**. The excellent fit of the model to T_m for these input changes is also shown in **Figure 8**. The testing sequence (not shown) fit the response as well as the training sequence.

The results of FBC with FFPC for the two disturbances is shown in **Figure 9**. The left plot is for FBC only. The right plot is FBC with announcements for T_{Ci} and C_{Ai}. As shown, the variation of T_m around its set point decreased greatly with FFC and announcements for both disturbances. More specifically, the standard deviation about the set point temperature dropped from 0.4352°C to 0.1131°C, a 74% reduction. Thus, modeling disturbances effectively and implementing them into FFC algorithms that can take advantage of announcements of future changes for critical disturbances can have a significant impact in reducing variation around the set point of CV.

6. FBPC and the Smith predictor

As demonstrated above, FBPC is an effective FBC strategy when θ_{MV} is large. The Smith Predictor (SP) [4, 9] is a widely accepted FBC strategy when there is no

deadtime in MV, and CV is measured, not at t, when MV changes, but at $t + \theta_{CV}$ (see **Figure 10**). The SP idea is to obtain a predictive model for CV with deadtime, remove the deadtime, and use this estimator in the feedback error term for CV at t. In **Figure 11** an example of a SP process is illustrated with a block diagram representing the process given in **Figure 10**. As shown in **Figure 11**, MV = $M(t)$ (M is the signal of MV) immediately affects CV = $B(t)$ (B is the signal of CV), but the sensor is at $B_1(t) = B(t\text{-}\theta_{CV})$. Thus, SP uses a prediction of CV at t with an MV that changes CV immediately. In contrast, FBPC uses a forecast prediction of CV at $t + \theta_{MV}$ when it takes a time of θ_{MV} for a change in MV to affect CV. Moreover, the SP does not use a forecast estimator and is not applicable to cases with deadtime in MV. However, this section will show that FBPC, using the forecasting estimator of CV at $t + \theta_{CV}$, gives the same result as the SP. Consequently, FBPC can be used in place of the SP. However, the opposite is not true. More specifically, the SP is not applicable when a change in MV has time delay in changing CV, whereas FBPC is applicable for this case.

For a **Figure 10** type process, the SP should compensate for the deadtime (i.e., reduce its effect) and respond quicker using an accurate estimate of B_t than using an accurate measurement of $B_{1,t}$. The block diagram for the SP [4, 9] shows feedback control using $CV_t = \hat{B}_t$ with bias correction (BC) to address measurement bias. BC is the current measurement of $B_{1,t} - \hat{B}_{1,t}$, where $\hat{B}_{1,t}$ is the estimated value of $B_{1,t}$.

Thus, in the SP block diagram,

$$e_t = Y_t^{set} - B_t - \left(B_{1,t} - \hat{B}_{1,t}\right) \tag{21}$$

Similarly, for FBPC,

$$e_t = Y_{t+\theta_{MV}}^{set} - \hat{B}_{1,t+\theta_{MV}} \tag{22}$$

The same simulated CSTR used above was used in this study to compare classical FBC, FBPC and the SP control algorithm with and without feedback correction. A

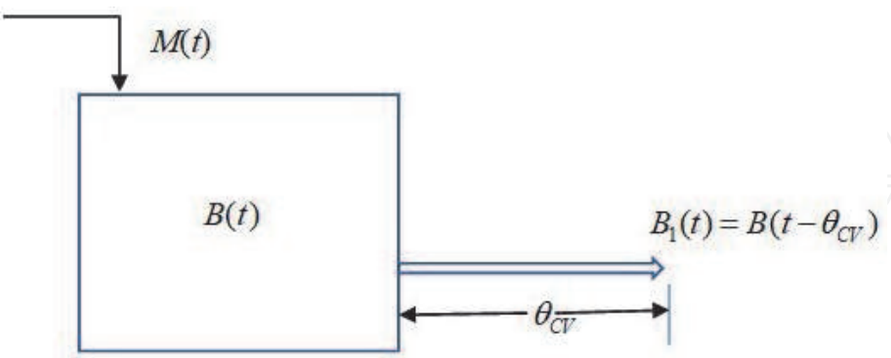

Figure 10.
An example of a SP process with M *as MV and* B_1 *as CV.*

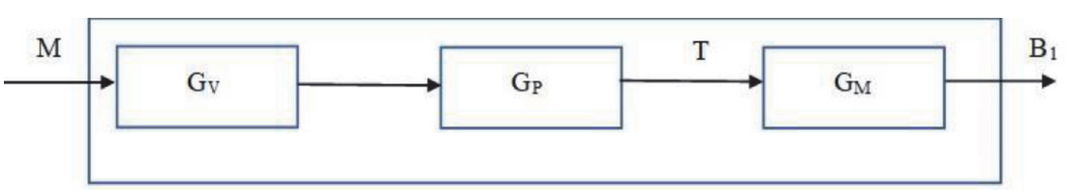

Figure 11.
A block diagram showing the blocks between M *and* B_1.

step test in M was done and obtained B_1 over time from the initial steady state to a final steady state. These values are: M_0 = 0.2569 and $M_\infty = 0.3800$ corresponding to B_{10} = 0.4000 and $B_{1,\infty} = 0.3800$. The input change was large enough to cover the change in T_m for the test data (i.e., a 4°C change in the set point temperature). A FOPDT model was fit to the data and the fitted response is given in **Figure 12**. As shown, the fit is excellent with the following estimates: $\hat{K} = 1.746$, $\hat{\tau} = 14.24\,s$ and $\hat{\theta} = 14\,s$ with $\hat{\delta} = \hat{\tau}/(\hat{\tau} + \Delta t) = 0.99303$ and Δt = 0.1. A plot of the response over time is given in **Figure 12**. The fitted forecast equation for $\hat{B}_{1,t+\theta_{MV}}$ is derived as follows:

$$\begin{aligned}
\tau\frac{dB_1'(t)}{dt} + B_1'(t) = KM'(t-\theta) \quad &\Rightarrow \tau\frac{B_{1,t}' - B_{1,t-\Delta t}'}{\Delta t} + B_{1,t}' = KM_{t-\theta-\Delta t}' \\
\vdots \quad &\Rightarrow (\tau + \Delta t)B_{1,t}' = \tau B_{1,t-\Delta t}' + K\Delta t M_{t-\theta-\Delta t}' \\
\Rightarrow B_{1,t}' = \frac{\tau}{\tau+\Delta t}B_{1,t-\Delta t}' + K\frac{\Delta t}{\tau+\Delta t}M_{t-\theta-\Delta t}' \quad &\Rightarrow B_{1,t}' = \delta B_{1,t-\Delta t}' + K(1-\delta)M_{t-\theta-\Delta t}' \\
\Rightarrow \hat{B}_{1,t+140} = B_{1,t}' + 0.4 = \hat{\delta}\hat{B}_{1,t+139} + \hat{K}\left(1-\hat{\delta}\right)M_{t-0.1} &
\end{aligned} \tag{23}$$

The SP estimate without BC is obtained from Eq. (23) as

$$\hat{B}_{t+140} = \hat{\delta}\hat{B}_{t+139} + \hat{K}\left(1-\hat{\delta}\right)M_{t-0.1} \tag{24}$$

With BC, the SP estimate is

$$\hat{B}_t = \hat{\delta}\hat{B}_{t-0.1} + \hat{K}\left(1-\hat{\delta}\right)M_{t-0.1} - \left(B_{1,t} - \hat{B}_{1,t}\right) \tag{25}$$

For a step change in the set point temperature of 4°C, the responses for tank temperature (T_m) for all four cases are given in **Figure 13**. The proportional-integral (PI) controller is the slowest to get to the new set point of 92°C. This is no surprise since the deadtime is quite large as shown in **Figure 12**. The SP with BC gives a modest improvement over PI which is surprising. This is also reflected in the

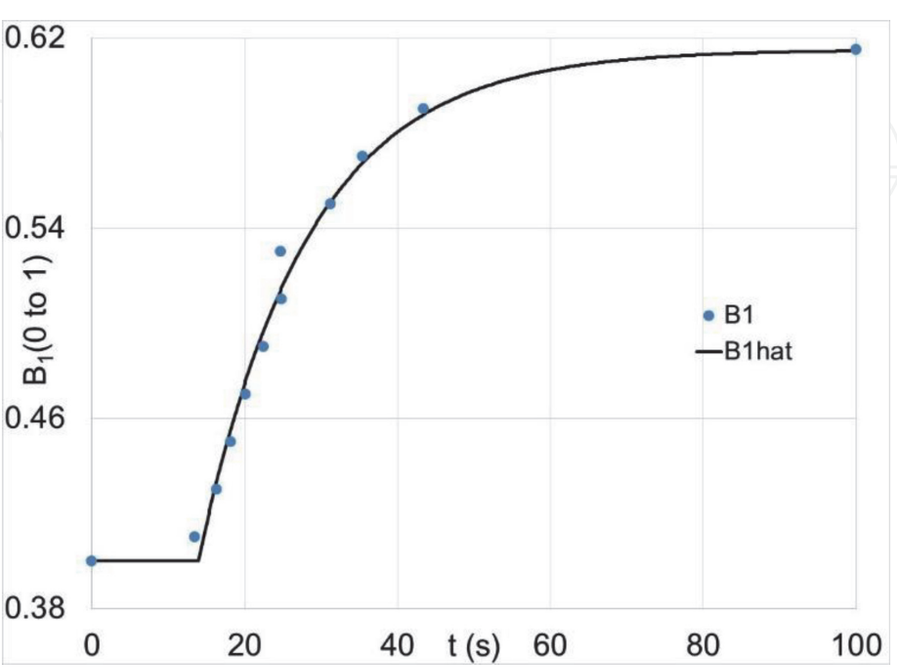

Figure 12.
The fitted process reaction curve of B_1 *the measured values used for the fitting for a step change in* M.

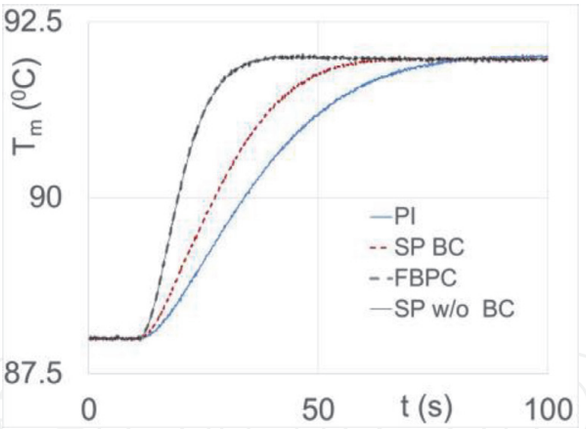

Figure 13.
Graphical SP results.

Controller	K_C	τ_I
PI	0.20	12.70
SP w BC	0.41	14.00
SP w/o BC	1.50	15.00
FBPC	1.50	15.00

Table 1.
Tuning values in the SP study.

modest increase in K_c from 0.20 to 0.41 as shown in **Table 1**. However, when the BC was removed, the SP response improved considerably as did K_c to 1.50. It gives the same response as FBPC, which also has no BC. These two cases give the same results, supporting the conclusion that FBPC and SP are equivalent for the SP application. However, when MV has deadtime with respect to CV, SP is not applicable, but FBPC is applicable. In [6] this BC method also did quite poorly with MPC being 132% worse (This BC method was not applied to FBPC in this study). Moreover, for BC, the following time series approach is recommended where the ϕ's are estimated with all other parameters for fitted model [6]:

$$\begin{aligned}\hat{y}_{t+\theta} &= \hat{\eta}_{t+\theta} + \hat{\phi}_1\left(y_t - \hat{\eta}_t\right) + \hat{\phi}_2\left(y_{t-\Delta t} - \hat{\eta}_{t-\Delta t}\right) + \cdots \\ &= \hat{\eta}_{t+k_1\Delta t} + \hat{\phi}_1 e_t + \hat{\phi}_2 e_{t-\Delta t} + \cdots\end{aligned} \tag{26}$$

7. Conclusions

This chapter has focused on the use of discrete-time dynamic forecast modeling to enhance FBC and all types of FFC. Discrete-time modeling has the advantage of obtaining solutions to PU systems without having to make assumptions to make the system an approximation of a physically realizable system. Models do not have to be *cause-and-effect* for forecasting but need to be as FFC models. Cause-and-effect models result from statistical design of experiments because input changes are orthogonal (i.e., uncorrelated) and for theoretical structured models because they will be nonlinear in one or more physically based parameters, have physical constraints that must be met, and physically interpretable unknown model parameters [23].

When MV has deadtime with-respects-to CV (e.g., θ_{MV}), a change in MV will not begin to change CV until a time distance of θ_{MV} in the future. Three FBC

approaches where evaluated in this scenario: classical FBC, FBPC and MPC, using the current measured value of CV, forecast estimate of CV, θ_{MV} in the future, and forecast estimate of CV, $\theta_{MV} + J\Delta t$ in the future, respectively. In the simulation study, FBC responded quicker than MPC when the process lag was large and MPC responded quicker when the process lag was small. FBPC responded much faster than both under small and large lag. FBPC control has a prediction horizon of θ_{MV} but for MPC it is $J\Delta t$ longer. Since the optimal value of J increases as the lag increases, MPC can be significantly more sluggish than FBPC when J is large. A definite advantage of MPC is that J is its only tuning parameter.

A discrete-time FFC approach (FFPC) was presented in this chapter that can be effective when θ_{MV} is large and the multiple-input FFPC model is PU for any reason (i.e., the order of the differential equation or negative deadtime). FFPC

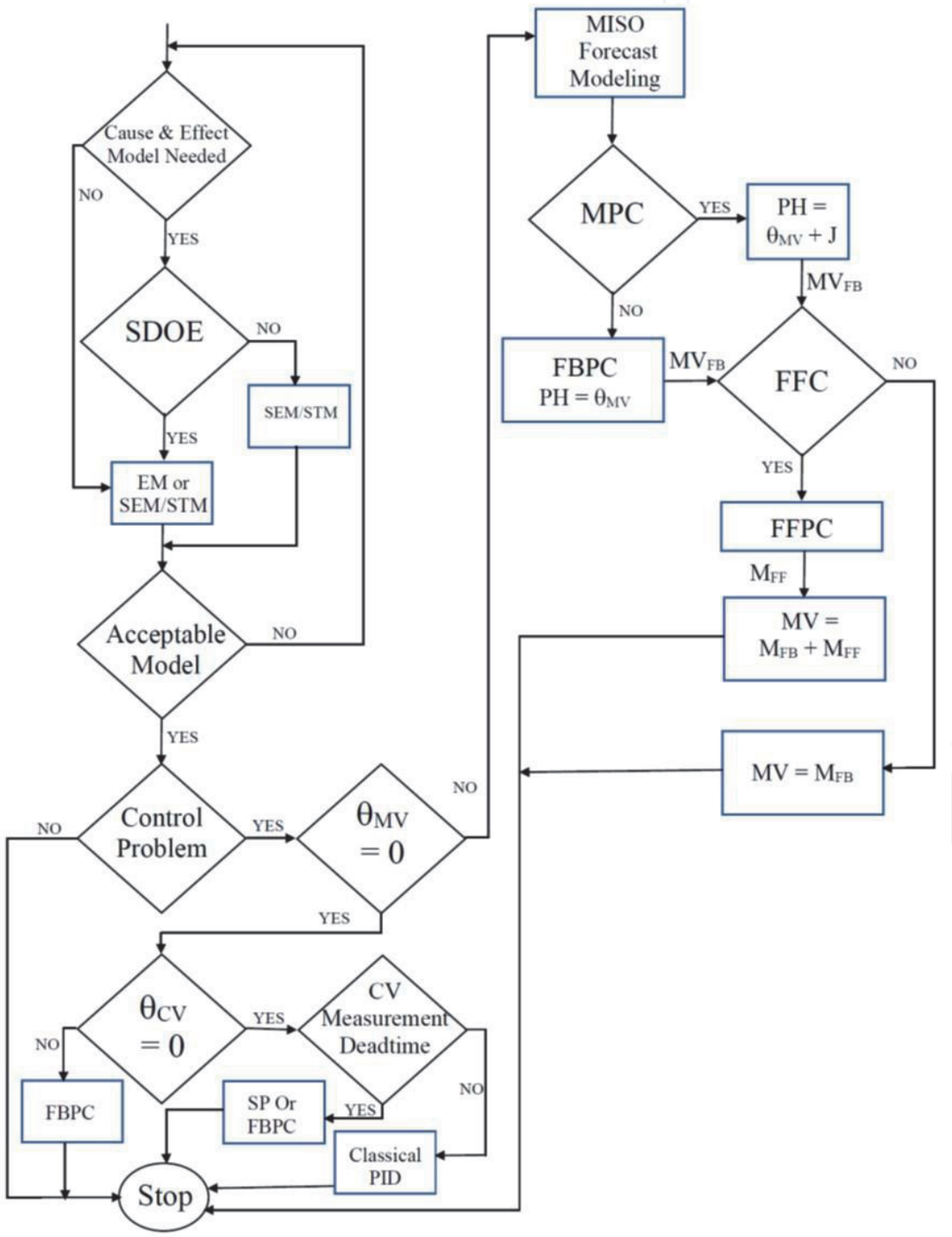

Figure 14.
Flowchart illustrating the complete process of the proposed framework of this chapter.

was shown to satisfy perfect theoretical control in a simulated data study. A critical strength of the approach presented in this work is that the FFC variables enter one mathematical function that simultaneously solves for one FFC control signal. This contrasts with classical FFC that has a FFC algorithm for each input and combines their values to determine the value of the FFC control signal for MV. The classical approach cannot treat complex interactive and nonlinear behavior of the disturbances in determining the optimal value of the FFC signal for MV. Block diagrams of this novel FFC approach were shown for the Wiener Network and a general block-oriented modeling approach. When FFC inputs have a PU impact, knowing how their values will change over the control horizon (i.e., announcements), can significantly improve FFC as demonstrated in the CSTR simulation study.

The SP is a model-based feedback control algorithm that can be quite effective when there is no deadtime between a change in MV and its impact on CV, and the measured value of CV has deadtime. For this situation, FBPC, that uses a forecast value for CV based on a model developed from the measured value of CV with deadtime, gives the equivalent result of the SP. However, the SP is limited to this case, but FBPC is not. More specifically, FBPC is applicable when there is deadtime for changes in MV and its effect on CV but the SP is not. Finally, one should exercise care when using the bias correction (BC) method in the block diagram for the SP. It can lead to a significantly suboptimal SP as shown in this work. A better alternative is to use one that is obtained from modeling the serially correlated structure in the process as given in this chapter. A flowchart illustrating the complete process of the proposed framework of this chapter is shown in **Figure 14**.

Acknowledgements

I thank Kendra Kreienbrink for helping with the references and for proofreading this document.

Nomenclature

A	cross-sectional area of the tank
a_n	the n^{th} constant
B	the signal of CV in the SP algorithm
BC	bias correction in the SP algorithm
B_1	the signal of CV with deadtime θ_{CV}
b_m	the m^{th} constant
C_{Ai}	inlet concentration to the CSTR (x_1)
e_{ffc}	the feedforward control law criterion for perfect control
e_t	the feedback error = $Y^{set} - y_t$,
F_C	inlet flow rate of the coolant to the jacket of the CSTR
$f(V^e)$	the true function in the FFC law that satisfy $e_{ffc} = 0$
$f(\boldsymbol{V})$	is an unrestricted mathematical function that maps each v_i' to the units of the output variable in standard form. Thus, it is $f(\boldsymbol{V})$ that transforms the linear dynamic inputs into the nonlinear dynamic response for the output y.
G_f	feedforward transfer function
G_{DV}	DV transfer function
G_i	transfer function with output v_i

G_M	transfer function for CV in signal
G_{MV}	MV transfer function
G_P	process transfer function
G_V	transfer function for MV
h	the tank level
J	the only controller tuning parameter for MPC.
K	process gain
K_C	controller gain for FBC
m	m^{th} order derivative
M	the input signal to MV transfer function
M_{FB}	FBC input signal to MV transfer function
M_{FF}	FFC input signal to MV transfer function
n	n^{th} order derivative
q_1	inlet flow rate of Stream 1
Q	flowrate in the Laplace domain entering the system
q	flow rate of the outlet stream
R_v	valve resistance
t	current time or just time
T	the physical value of CV in SP case
T_{Ci}	inlet temperature of the coolant to the jacket of the CSTR
T_m	measured tank temperature
v_i	dynamic output for i^{th} input, x_i, in the same units as x_i
$V(t)$	is a vector of the $v_i''s$
x	input
$x_{t\text{-}\Delta t}$	the value of x at time t -Δt
x_i'	deviation of x_i at time t from x_i at time t = 0
x_p^e	x_{MV}^e equals the value of MV in the FFC law that satisfy $e_{ffc} = 0$
y	the response = output
$\hat{y}(t)$	the estimate of $y(t)$

Greek Letters

θ	time delay or deadtime
$\eta(t)$	the true value of the output at time t
$\hat{\eta}(t)$	the estimate of $\eta(t)$
$\omega_{i,j}$	dynamic coefficient for the i^{th} input at $t - j\Delta t$
$\delta_{i,j}$	dynamic coefficient for output v_i at $t - j\Delta t$
θ_{CV}	dead time of the controlled variable
θ_{DV}	dead time of the disturbance variable
θ_{MV}	dead time of the manipulated variable
τ_I	reset time for FBC
τ	process time constant
Δt	the sample rate

Acronyms and Abbreviations

BGC	blood glucose concentration
CSTR	Continuous-Stirred-Tank-Reactor
CV	control variable
DT	deadtime
DV	disturbance variable
EM	empirical modeling

EMM	empirical modeling methods
FBC	feedback control
FBFFC	feedback/feedforward control
FBPC	feedback predictive control
FFC	feedforward control
FFPC	feedforward predictive control
FOPDT	first-order-plus-deadtime
MISO	multiple-input, single-output
MPC	model predictive control
MV	manipulated variable
PID	proportional, integral, derivative
PH	prediction horizon
PU	physically unrealizable
SEM	semi-empirical model
SDOE	statistical design of experiments
STM	semi-theoretical model
SP	Smith Predictor
SOPDT	second-order-plus-deadtime
TDPU	time delay physical unrealizability

Author details

Derrick K. Rollins
Department of Chemical, Biological Engineering and Statistics, Iowa State University, Ames, Iowa, USA

*Address all correspondence to: drollins@iastate.edu

References

[1] Mellodoge P. A Practical Approach to Dynamical Systems for Engineers. Ltd: Elsevier; 2016

[2] Tan L, Jiang L. Digital Signal Processing. 3rd ed. Inc: Elsevier; 2019

[3] Aldrich J. Correlations genuine and spurious in Pearson and Yule. Statistical Science. 1995;**10**(4):364-376

[4] Seborg, D, Edgar T, Mellichamp D. Process Dynamics and Control, 2nd edition, Wiley 2004.

[5] Smith C. Corripio A. Principles and Practice of Automatic Process Control: John Wiley & Sons; 1985

[6] Rollins D, Mei Y. A new feedback predictive control approach for processes with time delay in the manipulated variable. Chemical Engineering Research and Design. 2018; **136**:806-815

[7] García C, Prett D, Morari M. Model predictive control: theory and practice – a survey. Automatica. 1989;**25**(3): 335-348

[8] Quin S, Badgwell T. A survey of industrial model predictive control technology. Control Engineering Practice. 2003;**11**(7):733-764

[9] Smith O. Closer control of loops with dead time. Chemical Engineering Progress. 1957;**53**(5):217-219

[10] Huyett L, Dassua M, Zisser H, Doyle F. Design and evaluation of a robust PID controller for a fully implantable artificial pancreas. Industrial & Engineering Chemistry Research. 2015;**54**:10311-10321

[11] Rae-Puckett W. Dynamic modelling of diabetes mellitus [Dissertation]. Wisconsin-Madison: University of Wisconsin-Madison; 1992

[12] Noguchi C, Hashimoto S, Furutani E. In silico blood glucose control for type 1 diabetes with meal announcement using carbohydrate intake and glycemic index. Advanced Biomedical Engineering. 2016;**5**:124-131

[13] Clarke W, Anderson S, Breton M, Patek S, Kashmer L, Kovatchev B. Closed-loop artificial pancreas using subcutaneous glucose sensing and insulin delivery and a model predictive control algorithm: the Virginia experience. Journal of Diabetes Science and Technology. 2009;**3**(5):1031-1038

[14] Pearson R, Pottmann M. Gray-box identification of block-oriented nonlinear models. Journal of Process Control. 2000;**10**(4):301-315

[15] Rollins D, Bhandari N, Kleinedler J, Kotz K, Strohbehn A, Boland L, et al. Free-living inferential modeling of blood glucose level using only noninvasive inputs. Journal of Process Control. 2010;**20**:95-107

[16] Kotz K, Cinar A, Mei Y, Roggendorf A, Littlejohn E, Quinn L, et al. Multiple-input subject-specific modeling of plasma glucose concentration for feedforward control. Ind. Eng. Chem. Res. 2014;**53**(47):18216-18225

[17] Rollins D, Mei Y, Kotz K, Littlejohn E, Quinn L, Roggendorf A, et al. An extended static and dynamic feedback/feedforward control algorithm for insulin delivery in the control of blood glucose level. Ind. Eng. Chem. Res. 2015;**54**(26):6734-6748

[18] Cameron F, Niemeyer G, Bequette B. Extended multiple model prediction with application to blood glucose regulation. Journal of Process Control. 2012;**22**:1422-1432

[19] Bequette B. Algorithms for a closed-loop artificial pancreas: the case for

model predictive control. Journal of Diabetes Science and Technology. 2013; **7**(6):1632-1643

[20] Wang Q, Xie J, Molenaar P, Ulbrecht J. Model predictive control for type 1 diabetes based on personalized linear time-varying subject model consisting of both insulin and meal inputs: an in silico evaluation. J Diabetes Sci Technol, 2015; Jul, 9(4), 941-942.

[21] Marchetti G, Barolo M. and etc. A feedforward-feedback glucose control strategy for Type 1 Diabetes Mellitus. Journal of Process Control. 2008;**18**(2): 149-162

[22] Rollins D, Mei Y, Loveland S, Bhardari N. Block-oriented feedforward control with demonstration to nonlinear parametrized wiener modeling. Chemical Engineering Research and Design. 2016;**109**:397-404

[23] Rollins D, Roggendorf A, Khor Y, Mei Y, Lee P, Loveland S. Dynamic modeling with correlated inputs: theory, method and experimental demonstration. Ind. Eng. Chem. Res. 2015;**54**(7):2136-2144